Journal of Inclusion Phenomena and Macrocyclic Chemistry **34:** 331–343, 1999.

Out-of-Plane Motion of the Guest Benzene Molecule Trapped in a $[Cd(dmen)_2(CN)]_2[Cd(CN)_4]$ Host as Studied by ^{2}H-NMR

SHIN-ICHI NISHIKIORI*

Department of Basic Science, Graduate School of Arts and Sciences, The University of Tokyo, 3-8-1 Komaba, Meguro-ku, Tokyo 153-8902, Japan

(Received: 7 July 1998; in final form: 1 October 1998)

Abstract. An out-of-plane rotational motion of the guest benzene molecule trapped in a $[Cd(dmen)_2(CN)]_2[Cd(CN)_4]$ host, which is a cadmium cyano complex (dmen = *N*, *N*′-dimethyl-1,2-diaminoethane), was detected by means of ^{2}H-NMR powder patterns measured over a temperature range of 123–423 K. A simple inequivalent 8-site reorientation model which has two independent populations was used in the line shape simulation, and the potential trapping the benzene molecule was analyzed to be transformable depending on temperature. Structural flexibility of the host, which is considered to be a cause of the variable potential, was confirmed from the detection of a puckering-like motion of the dmen chelate ring that makes a part of the inner wall of the cavity trapping the guest benzene molecule.

Key words: cadmium cyano complex, benzene inclusion compound, ^{2}H-NMR, molecular motion

1. Introduction

Benzene is one of the most popular guest molecules of inclusion compounds and its motional behavior has been investigated in various inclusion compounds. It is well known that a guest benzene molecule is usually undergoing reorientation about its 6-fold axis, which is the in-plane motion, and much information on the in-plane motion has been obtained from many inclusion compounds [1, 2]. In some cases a guest benzene molecule has freedom towards the out-of-plane direction. In these cases, X-ray diffraction shows a disordered picture for the guest benzene molecule and structural information on the benzene molecules is difficult to obtain. Perhaps, solid NMR is the most useful method to elucidate the state of the guest benzene molecule under such conditions. However, there have been few studies focused on the out-of-plane motion of the guest benzene molecules [3, 4], and the information is not enough for us to discuss the motional behavior of guest benzene molecules from a viewpoint of out-of-plane motion. In this report one example of an out-of-

* Author for correspondence.

plane rotational motion of a guest benzene molecule and a useful motional model will be presented.

In this study the title benzene inclusion compound $[Cd(dmen)_2(CN)]_2[Cd(CN)_4]\cdot C_6H_6$ was chosen as a target. The compound was synthesized in the course of the structural development of inclusion compounds having a polycyanopolycadmate host [5, 6] and its crystal structure at room temperature was determined by Saito and Kitazawa [6]. The crystal structure is illustrated in Figure 1. The host of the inclusion compound is a one-dimensional infinite chain of the Cd complex $[Cd(dmen)_2(CN)]^+$, where each dmen(*N*, *N*′-dimethy-1,2-diaminoethane) is coordinating to equatorial positions of an octahedral cadmium to make a chelate ring and each cyano group makes a bridge between two adjacent $Cd(dmen)_2$ complexes by coordinating to the axial positions of the $Cd(dmen)_2$ complexes. Guest benzene molecules and isolated $[Cd(CN)_4]^{2-}$ anionic complexes are alternately aligned parallel to the chain of the $[—Cd(dmen)_2\text{-}CN—]_\infty$ one dimensional complex. The guest benzene molecules and $[Cd(CN)_4]^{2-}$ anions are on a $\bar{4}$ inversion axis of the crystal. The symmetry of the $[Cd(CN)_4]^{2-}$ anion is coincident to that of the $\bar{4}$ inversion axis. On the other hand, the molecular symmetry of the benzene molecule is not coincident to that of the $\bar{4}$ inversion axis, because the axis runs through the 1 and 4 positions of the benzene molecule. The X-ray diffraction analysis showed a disordered picture for the guest benzene molecule, where two very distorted benzene molecules were overlapped perpendicular to each other with very large thermal ellipsoids. From this result it is difficult to obtain meaningful information about the state of the guest molecule. However, an out-of-plane motion with large vibrational amplitude is expected for the guest benzene molecule, and it is a good target for a ^{2}H-NMR study.

2. Experimental

2.1. PREPARATION

The sample used in the NMR measurement was prepared by a method that was modified from Saito's original method [6] to obtain the pure compound. 0.89 g of $CdCl_2\cdot 5/2H_2O$ and 0.9 mL of dmen($CH_3NH—CH_2—CH_2—HNCH_3$) were added to 50 mL of 0.1 M $K_2[Cd(CN)_4]$ aq. soln. with stirring. The mixture was warmed until the white precipitate dissolved, and was stood at room temperature over night. After the precipitate was filtered, C_6D_6 (purchased from Merck, 99.5% D) was poured onto the surface of the filtrate. After two weeks, colorless crystals of $[Cd(dmen)_2(CN)]_2[Cd(CN)_4]\cdot C_6D_6$ were obtained. $[Cd(dmen\text{-}d_2)_2(CN)]_2[Cd(CN)_4]\cdot C_6H_6$, which contains dmen-$d_2$ ($CH_3ND—CH_2—CH_2—DNCH_3$) instead of normal dmen, was prepared by the above method using deuterated water and normal benzene instead of normal water and C_6D_6. The samples were identified by powder X-ray diffraction and IR spectroscopy.

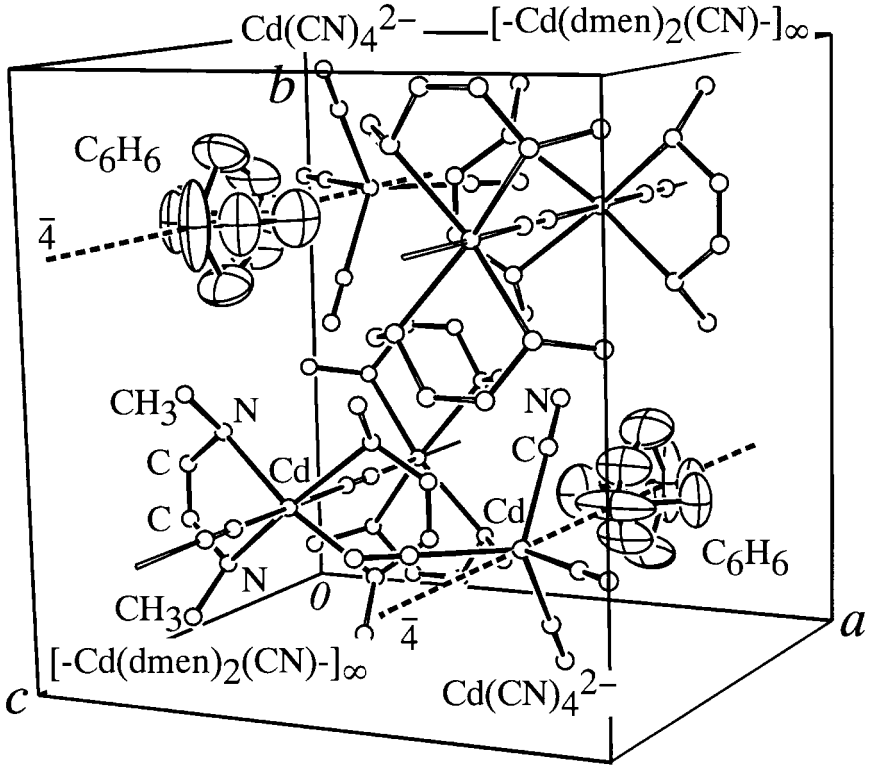

Figure 1. Crystal structure of $[Cd(dmen)_2(CN)]_2[Cd(CN)_4]\cdot C_6H_6$ at room temperature [6]. Hydrogen atoms are omitted for clarity. The C atoms of the benzene molecule are displayed with a thermal ellipsoid of a 30% probability and other atoms are displayed with a sphere of 0.15 Å radius. The benzene molecules and $[Cd(CN)_4]^{2-}$ anions are located on a $\bar{4}$ inversion axis of the crystal, which is indicated by a dashed line. The infinite chain of [—$Cd(dmen)_2(CN)$—] complexes is on a 4-fold screw axis, which parallels the $\bar{4}$ inversion axis. Crystal data: tetragonal, $P4_2/nmc$, a = 12.928(2) Å, c = 11.963(1) Å, V = 1999.5(6) Å^3, Z = 2.

2.2. MEASUREMENT OF ^{2}H-NMR POWDER PATTERNS

^{2}H-NMR powder patterns were measured at 45.6 MHz over a temperature range of 123–423 K using a Chemangetics CMX-300 NMR spectrometer equipped with a nitrogen gas flow sample temperature controller. The quadrupole echo pulse sequence [7] with a 90° pulse of 2 μs pulse width and interpulse spacings (τ) of 35 μs and 100 μs was applied. The recycle time was adjusted between 1 s and 30 s depending on T_1, and echo signals were accumulated until an appropriate S/N ratio was obtained. The observed patterns are shown in Figure 2 and Figure 5(a).

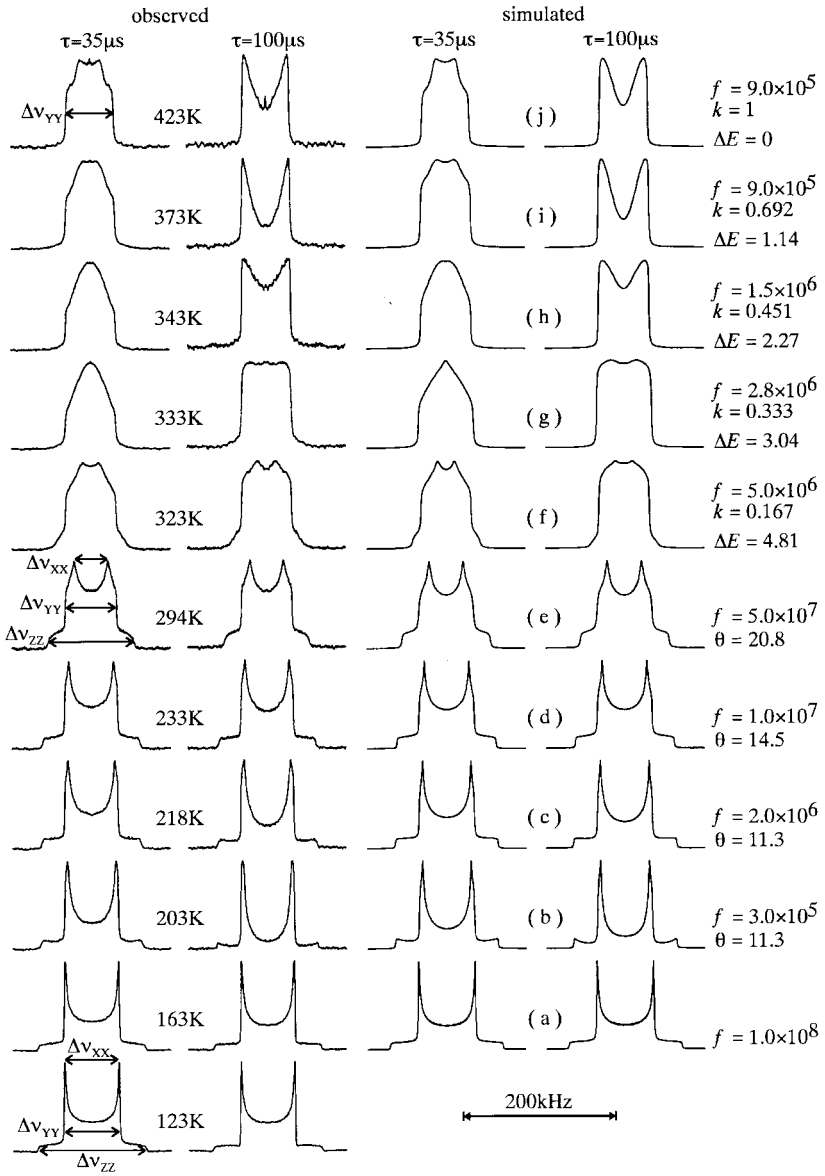

Figure 2. Observed and simulated ^{2}H-NMR powder patterns of $[Cd(dmen)_2(CN)]_2[Cd(CN)_4]\cdot C_6D_6$. Figure (a), (b)–(e), (f)–(i) and (j) are patterns simulated using the equivalent 6-site reorientation model, the 2-site reorientation model, the inequivalent and the equivalent 8-site orientation model, respectively. The jump frequency, the angle separating two sites in the 2-site reorientation model and the population of site-2 in the inequivalent 8-site reorientation model are indicated with f (s^{-1}), θ (°) and k, respectively. ΔE (kJ mol^{-1}) is the energy difference between site-1 and site-2 in the inequivalent 8-site reorientation model, which was calculated from the value of k and the equation of $k = \exp(-\Delta E/RT)$. Each pattern was normalized to be unit intensity.

2.3. CALCULATION OF THE SPECTRAL SPLITTINGS IN A FAST SPEED REGION AND LINE SHAPE SIMULATION

Before performing the line shape simulation of the ^{2}H-NMR powder patterns, the characteristic spectral splittings of a powder pattern in a fast motion region, where the jump frequency is more than 10^7 s^{-1}, were calculated. This calculation is rather easy and useful to estimate and examine a motional model. Some examples of the spectral splittings, $\Delta\nu_{XX}$, $\Delta\nu_{YY}$ and $\Delta\nu_{ZZ}$, are shown in Figure 2, and the procedure of the calculation is summarized in the Appendix. The line shape simulation of patterns in an intermediate speed region, where the jump frequency is 10^4 s^{-1}–10^7 s^{-1}, was carried out using a FORTRAN program written by the author [4] based on a previously published calculation principle [8, 9]. The calculation was carried out on a VIP6300ECD computer. The values for the quadrupole coupling constant in Hz(Qcc) and the asymmetry parameter(η) for benzene in a static state, 183 kHz and 0.04, respectively, were cited from the work of Ok and coworkers [2], because the motion of the guest benzene molecule did not reach a static state and the values for those parameters were not obtained experimentally in this measurement. The simulated line shapes are shown in Figure 2(a)–(j) and Figure 5(b).

3. Results and Discussion

Figure 2 shows measured ^{2}H-NMR powder patterns of the deuterated benzene inclusion compound. The measurement was carried out with two interpulse spacings, τ = 35 μs and τ = 100 μs, to ensure the line shape simulation. The patterns at 123 K and 163 K are very similar and they are axial patterns in a fast speed region. These axial patterns show the guest benzene molecule is undergoing a rotational motion where the six deuterium atoms are equivalent. To satisfy those conditions, a reorientation about the 6-fold axis of the benzene molecule, which is the so-called in-plane rotational motion of benzene, is the most natural model. Here, the most popular equivalent 6-site reorientation is assumed. The model is illustrated in Figure 3(a). The direction of the electric field gradient tensor at each site in the reference frame was described using the Euler angles as follows: $\alpha_i = 60i - 30°$ for site-i; β_i = 90°, γ_i = 90°, and p_i = 1 were common for all the sites (i = 1–6). The definition of the Euler angles used here is in accordance with that used in a previous work [4]. Under these conditions, the electric field gradient tensor averaged by the 6-site reorientation is already a diagonal matrix

$$\frac{-eq}{2}\begin{pmatrix} \frac{-1}{2}(1+\eta) & 0 & 0 \\ 0 & \frac{-1}{2}(1+\eta) & 0 \\ 0 & 0 & 1+\eta \end{pmatrix}$$

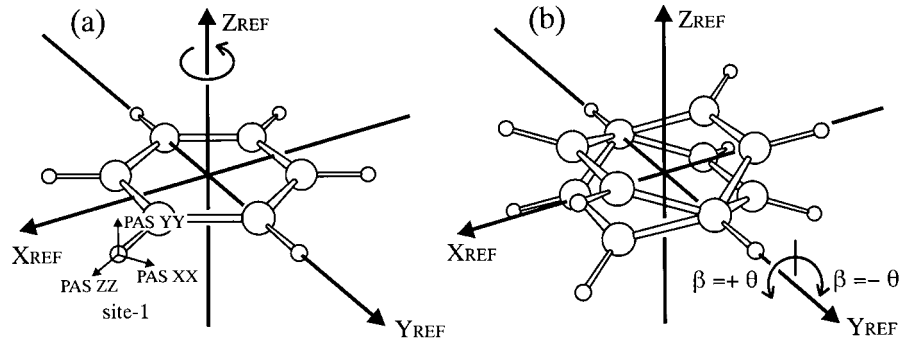

Figure 3. (a) Equivalent 6-site reorientation model and the reference frame ($X_{\mathrm{REF}}Y_{\mathrm{REF}}Z_{\mathrm{REF}}$). The benzene ring is on the $X_{\mathrm{REF}}Y_{\mathrm{REF}}$ plane, and is undergoing a 6-site reorientation about the Z_{REF} axis. The principal axis system of the electric field gradient tensor at site-1 is illustrated, where $\alpha_1 = 30°$, $\beta_1 = 90°$, $\gamma_1 = 90°$. The definition of the Euler angles here accords with that in a previous work [4]. (b) 2-site reorientation model and equivalent/inequivalent 8-site reorientation model. Above 163 K, the benzene molecule undergoing a fast 6-site reorientation begins another reorientation about an axis perpendicular to the 6-fold axis. This motion is modeled as a reorientation about the Y_{REF} axis of the benzene ring under the conditions of (a). In the 2-site reorientation, the benzene ring undergoes a reorientation between two sites that are separated by an angle 2θ about the Y_{REF} axis. In the equivalent/inequivalent 8-site reorientation model, the benzene ring undergoes a rotational reorientation between eight sites that are separated by 45° from each other about the Y_{REF} axis.

and spectral splittings are calculated to be 71 kHz, 71 kHz and 142 kHz as shown in the Appendix. They agree well with the observed values, 70(1) kHz, 70(1) kHz and 140(1) kHz, within their observational errors. The result of this calculation suggests that no out-of-plane motion takes place in this temperature region. The line shapes simulated based on the 6-site reorientation model are shown in Figure 2(a).

At 203 K and at 218 K, some differences were recognized between the observed patterns measured with the two interpulse spacings in their shape and intensity. This observation indicates the patterns are those in an intermediate speed region. Consequently, another motion combined with the fast in-plane motion begins between 163 K and 203 K. Above 203 K, the spectral splittings $\Delta\nu_{XX}$ and $\Delta\nu_{ZZ}$ changed gradually with increasing temperature as shown in Figure 2. However, the spectral splittings $\Delta\nu_{YY}$ was almost constant up to 423 K. These findings suggest that an out-of-plane motion about an axis perpendicular to the 6-fold axis of the benzene molecule takes place. The constant $\Delta\nu_{YY}$ also strongly suggests the axis for the out-of-plane motion is fixed over the observed temperature range. This is a remarkable point for the molecular motion of this guest benzene molecule. It, perhaps, comes from the crystal structure formed with the arrangement of the linear host complexes.

Around 203 K, the decrease of $\Delta\nu_{XX}$ and $\Delta\nu_{ZZ}$ was not so large. It is appropriate that the out-of-plane motion is a reorientational motion within a narrow area.

The simplest model is a 2-site reorientation model, where the benzene molecule in the fast in-plane motion is undergoing a reorientation between two sites about an axis perpendicular to the 6-fold axis of the benzene molecule. It is a natural idea that the axis for the out-of-plane motion coincides with the $\bar{4}$ inversion axis of the crystal, which is perpendicular to the 6-fold axis of the benzene molecule in the crystal structure at room temperature. Considering that the principal axes of the electric field gradient tensor averaged by the fast in-plane motion are coincident with those of the reference frame of Figure 3(a), this 2-site reorientational motion is modeled as the reorientation of the averaged electric field gradient tensor between two sites, which are separated by an angle 2 θ about the Y_{REF} axis of the reference frame as shown in Figure 3(b). Each direction of the two sites is as follows: $\beta_1 = +\theta$ for site-1, $\beta_2 = -\theta$ for site-2; $\alpha_i = \gamma_i = 0$, $p_i = 1$ are common for the both sites ($i = 1, 2$). The electric field gradient tensor averaged by this 2-site reorientation is already diagonalized to be

$$\frac{-eq}{2}\begin{pmatrix} \frac{1}{4}(1+\eta)(1-3\cos 2\theta) & 0 & 0 \\ 0 & \frac{-1}{2}(1+\eta) & 0 \\ 0 & 0 & \frac{1}{4}(1+\eta)(1+3\cos 2\theta) \end{pmatrix}$$

These principal values show that $\Delta\nu_{YY}$ is constant and $\Delta\nu_{XX}$ and $\Delta\nu_{ZZ}$ depend on the angle θ. For simulating the patterns, the angle θ was assumed to be 11.3°, and the jumping frequency was assumed to be 3×10^5 s^{-1} and 2×10^6 s^{-1} for 203 K and 218 K, respectively. The simulated patterns are shown in Figure 2(b) and 2(c).

At 233 K and 294 K, patterns in a fast speed region were observed. The frequency of the 2-site reorientation reaches a frequency more than 10^7 s^{-1}. But their $\Delta\nu_{XX}$ and $\Delta\nu_{ZZ}$ were narrower than those at 203 K and 218 K. Assuming the 2-site reorientational motion, the angle θ was calculated to be 14.5° for 233 K and 20.8° for 294 K. The simulated patterns in Figure 2(d) and 2(e) were calculated with $f = 1 \times 10^7$ s^{-1} and 5×10^7 s^{-1}, respectively.

Above 323 K the observed patterns showed features of patterns in an intermediate speed region, again. Above 423 K fast limit line shapes were not observed, because just above 423 K the decomposition of the compound accompanied with release of the benzene began. Looking at the observed patterns, it could be imagined that around 333 K $\Delta\nu_{XX}$ is near 0 kHz and at 423 K $\Delta\nu_{XX}$ increases to half of $\Delta\nu_{YY}$. This change of the spectral splittings can be explained using the 2-site reorientation model on the assumption that the angle θ increases depending on temperature as shown in the above case. However, the line shapes above 323 K could not be reproduced by the line shape simulation based on the 2-site reorientation model. Presumably a motion of another type begins between 294 K and 323 K. If the line shape at 423 K is an axial pattern, where $\Delta\nu_{XX}$ is half of $\Delta\nu_{YY}$, in an intermediate speed region, it is natural that the out-of-plane motion at 423 K

is a rotational motion rather than a reorientational motion within a limited area. Such a rotational motion is supported by information of the crystal structure at room temperature. The void space in the cavity is large enough for the benzene molecule to undergo a rotational motion about the $\bar{4}$ inversion axis. Considering the crystal structure, the first choice for the rotational motion at 423 K is an equivalent 4-site reorientation. The Euler angles for the equivalent 4-site reorientation in the reference frame of Figure 3(b) are as follows: $\beta_i = 90(i-1)^\circ$ for site-i; $\alpha_i = \gamma_i = 0^\circ$ and p_i = 1 for all the sites (i = 1–4). However, this equivalent 4-site reorientation model was discarded. The equivalent 4-site reorientation, in which several intermediate jump frequencies were tried, did not reproduce the observed patterns. Then, other equivalent n-site reorientation models, where n was a number between 2 and 8, were tried, because the rotational motion seems to be affirmed from the crystal structure. The Euler angles for the equivalent n-site reorientation are $\beta_i = 360(i-1)/n^\circ$ for site-i; $\alpha_i = \gamma_i = 0^\circ$ and p_i = 1 for all the sites ($i = 1-n$). After all, the observed patterns were reproduced in the cases of n = 3, 5, 6, 7 and 8. Considering the crystal structure, an equivalent 8-site reorientation is the most appropriate among the models. The simulated patterns using the equivalent 8-site reorientation model are shown in Figure 2(j). They agree with the observed patterns.

The gradual change of spectral splittings $\Delta\nu_{XX}$ and $\Delta\nu_{ZZ}$ over the measured temperature range suggests a change of the potential which traps the benzene molecule, depending on temperature. Below 423 K we must consider that the 8-fold symmetry is lowered to reproduce the observed non-axial line shapes. There are many ways to modify the potential, but it is very difficult to pick the true one. Here one of the simplest models will be presented. One possible and easy way to lower the 8-fold symmetry is to change the population at each site of the equivalent 8-site reorientation model depending on temperature, namely an inequivalent 8-site reorientation model. The location of each site is the same as that in the equivalent 8-site reorientation. As the inequivalent populations, three independent populations, p_1, p_2 and p_3, and an assumption that $p_1 = p_5$, $p_2 = p_4 = p_6 = p_8$ and $p_3 = p_7$, are considered. The actual independent parameters are reduced to two parameters, k_2 and k_3, where $k_2 = p_2/p_1$ and $k_3 = p_3/p_1$ ($0 \leq k_2, k_3 \leq 1$) and we can consider p_1 is always 1. Moreover, to reduce the number of frequency parameters, it is assumed that the energy barrier (E_a) from site-2 to site-1 and that from site-2 to site-3 have the same value. Therefore, the number of independent frequency parameters is only one, which is the frequency f for jumps from site-2 to site-1 and from site-2 to site-3. Even under these conditions, there are three parameters to be considered, k_2, k_3 and f, and the number of possible combinations of the parameters is enormous. Therefore, one more assumption is adopted, which is $k_2 = k_3 = k$. The potential profile of this simplified inequivalent 8-site reorientation model is illustrated in Figure 4. Based on the above conditions, the averaged electric field gradient tensor is calculated to be

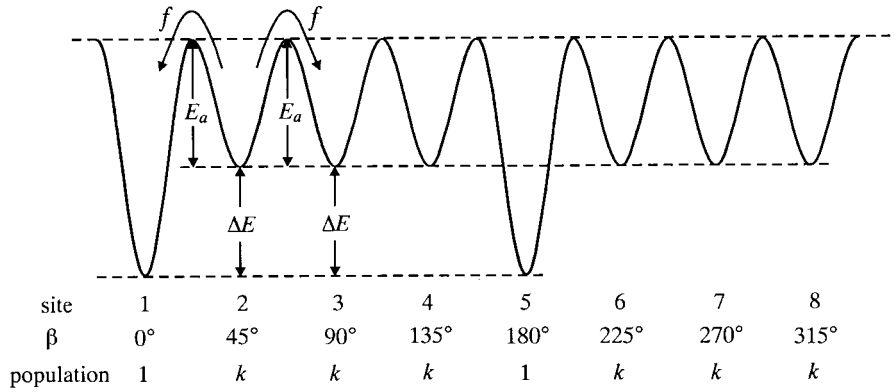

Figure 4. Potential profile of the simplified inequivalent 8-site reorientation model.

$$\frac{-eq}{2}\begin{pmatrix} \frac{1}{2}(1+\eta)\frac{3k-1}{3k+1} & 0 & 0 \\ 0 & \frac{-1}{2}(1+\eta) & 0 \\ 0 & 0 & \frac{1}{2}(1+\eta)\frac{2}{3k+1} \end{pmatrix}.$$

This result satisfies the change of $\Delta\nu_{XX}$ and $\Delta\nu_{ZZ}$ depending on k and the invariable $\Delta\nu_{YY}$. Needless to say, in the case of $k = 1$, which means $p_1 = p_2 = p_3$, it is the equivalent 8-site reorientation model. For reproducing the observed patterns, k was scanned in the range from 0 to 1, and f was scanned in the range from 10^4 s^{-1} to 10^7 s^{-1}. The best-fit results and parameters used are shown in Figure 2(f)–2(i). They are in good agreement with the observed ones. The inequivalent 8-site reorientation model works relatively well in spite of the considerable simplifications.

In contrast to the above case, the inequivalent 8-site reorientation model did not work well for the patterns observed at 203 K and 218 K. Their line shapes, especially those measured with the interpulse spacing of 100 μs, were not reproduced by the inequivalent 8-site reorientation model. This indicates that the motion is different between below 218 K and above 323 K: the 2-site reorientation within a narrow area takes place in the lower temperature region, and the inequivalent 8-site reorientation takes place in the higher temperature region. The pattern observed at 294 K is also interpretable using the inequivalent 8-site reorientation model. The parameters of $k = 0.068$ and $f = 2 \times 10^7$ s^{-1} give the best-fit results. However, it is impossible to judge which model is better, the 2-site reorientation model or the inequivalent 8-site reorientation model, because a fast limit pattern does not show a characteristic line shape depending on a motional mode. At this stage, the reorientational motion within a narrow area seems to be gradually excited to the rotational motion between 218 K and 323 K, but it is not clear where the motional mode

changes. In this NMR measurement no sign of a phase transition was observed. To obtain more detailed information about this point other techniques are necessary.

On the basis of the results of the simulation, the frequency of the molecular motion tends to decrease with increasing temperature above 294 K. This finding suggests the energy barrier (E_a) is not constant. Moreover, the change of k indicates the change of the energy difference (ΔE) between site-1 and site-2. Consequently, the whole potential trapping the benzene molecule changes depending on the temperature. The value of ΔE at each temperature could be calculated from the value of k and the Boltzmann distribution, and is shown in Figure 2(f)–2(j). Its results show that ΔE changes monotonously and smoothly. However, it is impossible to derive the value of E_a from the Arrhenius plot in this case, so that the details of the potential curve cannot be deduced.

The change of the potential means a structural change or fluctuation of the cavity. To seek evidence for such structural flexibility of the cavity, the possibility of a puckering motion of dmen was examined. Dmen makes the inner wall of the cavity, in which the methyl groups in particular have large contact with the guest benzene molecule. Therefore, the state of dmen greatly influences the motional behavior of the guest benzene molecule. The crystal structure at room temperature shows that the site symmetry at the Cd atom of the [Cd(dmen)$_2$(CN)] complex is 2mm. Therefore, dmen which makes a gauche form chelate ring must be in a static or a dynamic disordered state. The puckering motion of a five-membered chelate ring is well known in coordination chemistry [10]. In this inclusion compound a similar puckering motion of dmen was expected. Figure 5(a) shows ^{2}H-NMR powder patterns measured on [Cd(dmen-d_2)$_2$(CN)]$_2$[Cd(CN)$_4$]·C$_6$H$_6$ in which the hydrogen atom at the secondary amino group of dmen was replaced with a deuterium atom. The powder patterns showed line shapes from a near static state to a fast speed state through an intermediate speed region. In the puckering motion of this Cd complex, the motion of the deuterium atom is approximated to a 2-site reorientational motion about the Cd—N axis as shown in Figure 5(c). The best-fit results of the line shape simulation based on this simple 2-site reorientation model are shown in Figure 5(b). The parameters used in the best-fit results were as follows: the Euler angles describing each direction of the two sites are $\alpha = \pm 12.7°$, $\beta = 109.5°$ (the tetrahedral angle), $\gamma = 90°$ and p = 1; the Qcc and η in a static state are 202 kHz and 0.14 which were estimated from the pattern at 173 K. The jump frequencies are shown in Figure 5(b). The values of α are considered to be reasonable structurally because they were in good accord with the values of +13.6° and −12.7° that were estimated from a molecular mechanics calculation [11]. The simulated spectra agreed with the observed ones, and a puckering-like motion of dmen is confirmed. From the Arrhenius plot of log f (jump frequency) *vs.* $1/T$ the activation energy for the puckering-like motion was estimated to be 58(7) kJ mol^{-1}.

A plot of the quadrupole echo amplitude as a function of temperature is sometimes used to investigate molecular motions, because the echo amplitude is related to the rate of molecular motions [2, 8, 9]. In this case there was good correla-

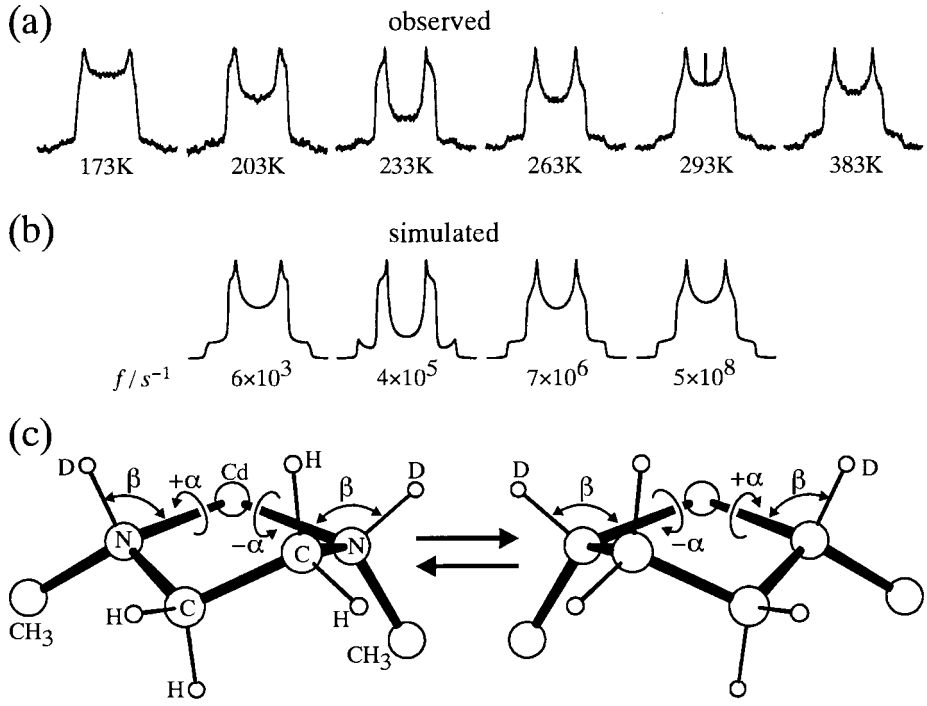

Figure 5. Observed (a) and simulated (b) ^{2}H-NMR powder patterns of $[Cd(dmen\text{-}d_2)_2(CN)]_2[Cd(CN)_4]\cdot C_6H_6$. (dmen-$d_2$ = $CH_3ND—CH_2—CH_2—DNCH_3$). The measurement was carried out with an interpulse spacing of 35 μs. (c) A model of the puckering motion of the dmen-d_2 chelate ring. The motion of the D atom of dmen-d_2 is approximated to a 2-site reorientation about the Cd—N bond. Parameters used in the simulation of (b) are as follows: $\alpha = +12.7°$ and $-12.7°$ for site-1 and site-2, respectively; β = 109.5°, $\gamma = 90°$, p = 1 for both the sites, and jump frequency is shown in (b).

tion between the plot for dmen and that for the guest benzene molecule in the temperature range of 123–203 K. The puckering-like motion of dmen and the 2-site reorientation of the benzene molecule seem to be activated at the same time. Above 203 K their correlation was lost. Probably, the rotational motion of the guest benzene molecule in the higher temperature region influences the echo amplitude of the benzene molecule. At this stage, it is a difficult problem to know how the motion of dmen is precisely correlated to the state of the guest benzene molecule.

4. Appendix: Calculation of the Spectral Splittings in a Fast Speed Region

The main principle of the calculation of the spectral splittings in a fast speed region is to obtain the principal values of an electric field gradient tensor averaged by a molecular motion [9, 12]. An electric field gradient tensor in a static state de-

scribed in a principal axis system, V_{PAS}, is written in (1), where η is the asymmetry parameter ($0 \leq \eta \leq 1$).

$$V_{\mathrm{PAS}} = \frac{-eq}{2} \begin{pmatrix} 1-\eta & 0 & 0 \\ 0 & 1+\eta & 0 \\ 0 & 0 & -2 \end{pmatrix} \tag{1}$$

The spectral splittings $\Delta\nu_{ii}$ ($ii = xx, yy, zz$) are proportional to the principal values of V_{PAS} as shown in (2), where Qcc is the quadrupole coupling constant in Hz.

$$\Delta\nu_{XX} = \frac{3}{4}Qcc|1-\eta|, \Delta\nu_{YY} = \frac{3}{4}Qcc|1+\eta|, \Delta\nu_{ZZ} = \frac{3}{4}Qcc|-2| \tag{2}$$

A reference frame is set to describe the direction of V_{PAS} in a molecular motion. The direction of a D—X bond is coincident with the Z principal axis of V_{PAS}. When a D atom visits n sites with population p_i at the ith site during a molecular motion, the averaged electric field gradient tensor $\bar{V}$ is described in (3). R is a rotation matrix described using the Euler angles α, β and γ, which indicate the direction of V_{PAS} at each site in the reference frame.

$$\bar{V} = \sum_{i=1}^{n} p_i \, {}^{t}R(\alpha_i, \beta_i, \gamma_i) V_{\mathrm{PAS}} R(\alpha_i, \beta_i, \gamma_i) \Big/ \sum_{i=1}^{n} p_i \tag{3}$$

Then, $\bar{V}$ is diagonalized to be $\bar{V}_{\mathrm{PAS}}$.

$$\bar{V}_{\mathrm{PAS}} = \frac{-eq}{2} \begin{pmatrix} \bar{V}_{\mathrm{PAS}XX} & 0 & 0 \\ 0 & \bar{V}_{\mathrm{PAS}YY} & 0 \\ 0 & 0 & \bar{V}_{\mathrm{PAS}ZZ} \end{pmatrix} \tag{4}$$

The spectral splittings in the fast molecular motion are proportional to the principal values of $\bar{V}_{\mathrm{PAS}}$, namely $\Delta\nu_{ii} = 3/4Qcc|\bar{V}_{\mathrm{PAS}ii}|$.

Acknowledgements

The author is indebted to Mr. Takashi Saito and Prof. Takafumi Kitazawa, Toho University, for providing the information of the preparation and the structural data of the benzene inclusion compound. This work was supported by a Grant-in-Aid for Scientific Research (C) Project No. 09640596 from the Ministry of Education, Science, Sports and Culture of Japan.

References

1. (a) B. G. Silbernagel, A. R. Garcia, J. M. Newsam, and R. Hulme: *J. Phys. Chem.* **93**, 6506 (1989). (b) S. Nishikiori, C. I. Ratcliffe, and J. A. Ripmeester: *J. Phys. Chem.* **95**, 1589 (1991).

(c) A. E. Aliev, K. D. M. Harris, and F. Guillaume: *J. Phys. Chem.* **99**, 1156 (1995), and references therein. (d) C-H. Kim, T. Soma, S. Nishikiori, and T. Iwamoto: *Chem. Lett.* **1996**, 89. (e) K. Ochiai, Y. Mazaki, S. Nishikiori, K. Kobayashi, and N. Hayashi: *J. Chem. Soc., Perkin Trans. 2* **1996**, 1139.

2. J. H. Ok, R. R. Vold, R. L. Vold, and M. C. Etter: *J. Phys. Chem.* **93**, 7618 (1989).
3. (a) E. Meirovitch, I. Belsky, and S. Vega: *J. Phys. Chem.* **88**, 1522 (1984). (b) G. A. Facey, C. I. Ratcliffe, and J. A. Ripmeester: *J. Phys. Chem.* **99**, 12249 (1995).
4. S. Nishikiori, T. Soma, and T. Iwamoto: *J. Incl. Phenom.* **27**, 233–243 (1997).
5. (a) T. Kitazawa, S. Nishikiori, and T. Iwamoto: *Material Sci. Forum.* **91–93**, 257 (1992). (b) T. Iwamoto, T. Kitazawa, S. Nishikiori, and R. Kuroda: in P. Bernier, J. E. Fischer, S. Roth and S. A. Solin (eds.), *Chemical Physics of Intercalation II*, Vol. 305, NATO ASI series B, Plenum Press (1993), pp. 325–332. (c) T. Kitazawa, S. Nishikiori, and T. Iwamoto: *J. Chem. Soc., Dalton Trans.* **1994**, 3695 (1994). (d) T. Iwamoto, S. Nishikiori, and T. Kitazawa: *Supramol. Chem.* **6**, 179 (1995).
6. T. Saito: BS. thesis for Toho University (1996). T. Saito and T. Kitazawa: Private communication.
7. (a) I. Solomon: *Phys. Rev.* **110**, 61 (1958). (b) J. H. Davis, K. R. Jeffery, M. Bloom, M. I. Valic, and T. P. Higgs: *Chem. Phys. Lett.* **42**, 390 (1976).
8. (a) H. W. Spiess and H. Sillescu: *J. Magn. Reson.* **42**, 381 (1981). (b) A. J. Vega and Z. Luz: *J. Chem. Phys.* **86**, 1803 (1987). (c) M. S. Greenfield, A. D. Ronemus, R. L. Vold, R. R. Vold, P. D. Ellis, and T. E. Raidy: *J. Magn. Reson.* **72**, 89 (1987).
9. (a) R. J. Wittebort, E. T. Olejniczak, and R. G. Griffin: *J. Chem. Phys.* **86**, 5411(1987). (b) T. M. Alam and G. P. Drobny, *Chem. Rev.* **91**, 1545 (1991)
10. (a) J. L. Sudmeire and G. L. Blackmer: *Inorg. Chem.* **10**, 2010 (1971). (b) J. L. Sudmeire, G. L. Blackmer, C. H. Bradley, and F. A. L. Anet: *J. Am. Chem. Soc.* **94**, 757 (1972). (c) R. E. Cramer and R. L. Harris: *Inorg. Chem.* **13**, 2208 (1974), and references therein. (d) S. Koner, A. Ghosh, N. R. Chaudhuri, A. K. Mukherjee, M. Mukherjee, and R. Ikeda: *Polyhedron* **12**, 1311 (1993). (e) R. Ikeda, K. Kotani, H. Ohki, S. Ishimaru, K. Okamoto, and A. Ghosh: *J. Mol. Struct.* **345**, 159 (1995).
11. Molecular modeling software, CAChe. Oxford Molecular Group Inc., (1996). N. L. Allinger's standard MM2 force field is used for molecular mechanics calculations. N. L. Allinger: *J. Am. Chem. Soc.* **99**, 8127 (1977)
12. R. G. Barnes: in J. A. S. Smith (ed.), *Advances in Nuclear Quadrupole Resonance*, Vol. 1, Heyden & Sons Ltd. (1974), pp. 335–355, .